

Temporal disorder does not forbid discontinuous absorbing phase transitions in low dimensional systems

M. M. de Oliveira¹ and C. E. Fiore²

¹*Departamento de Física e Matemática, CAP, Universidade Federal de São João del Rei, Ouro Branco-MG, 36420-000 Brazil,*

²*Instituto de Física, Universidade de São Paulo, São Paulo-SP, 05314-970, Brazil*

(Dated: January 17, 2019)

Distinct works have claimed that spatial (quenched) disorder can suppress the discontinuous absorbing phase transitions. Conversely, the scenario for temporal disorder for discontinuous absorbing phase transitions is unknown. In order to shed some light in this direction, we tackle its effect in three bidimensional examples, presenting undoubtedly discontinuous absorbing phase transitions. Except in one case (to be explained further), the temporal disorder is introduced by allowing the control parameter to be time dependent $p \rightarrow p(t)$ according to a uniform distribution of mean p_0 and width σ , in which at the emergence of the phase transition the system transits between active and absorbing regimes. In contrast to the spatial disorder, numerical results strongly suggest that temporal disorder does not forbid the existence of discontinuous transition. All cases are signed by behaviors similar to their pure (without disorder) counterparts, including bistability around the coexistence point and common finite size scaling behavior with the inverse of the system volume, as recently proposed in Phys. Rev. E. **92**, 062126 (2015). We also observe that temporal disorder does not induce temporal Griffiths phases around phase transitions, at least for $d = 2$.
PACS numbers: 05.70.Ln, 05.50.+q, 05.65.+bx

I. INTRODUCTION

In the last years, equilibrium and nonequilibrium phase transitions have been commonly employed for establishing the key features of a countless number of phenomena, such as magnetic systems, water-like anomalies, biological, ecological models and many others [1–4]. Recently, a considerable interest has been devoted to the inclusion of more realistic ingredients in order to describe (or mimicking) the effect of impurities or even external fluctuations as well as their effects in the phase transition [5–10].

Commonly, these ingredients are considered by allowing the control parameters to assume distinct values in the space or in the time. The former case, regarded as quenched disorder, affects drastically the phase transitions, leading to the existence of new universality classes and local regions in the absorbing phase characterized by large activity with slow decay toward the extinction. These rare regions are typically located for activation rates λ between the clean value λ_c^0 (without disorder) and the disordered critical point λ_c ($\lambda_c^0 < \lambda < \lambda_c$) and present non-universal exponents [11–13]. Heuristically, the relevance of quenched disorder can be understood by means of the Harris criterion [14], that establishes that it is a relevant perturbation whenever $d\nu_\perp < 2$, being d the system dimensionality and ν_\perp the spatial correlation length exponent. Since for models belonging to the directed percolation (DP) universality class ν_\perp read $\nu_\perp = 1.096854(4), 0.734(4)$ and $0.581(5)$ in $d = 1, 2$ and 3 , respectively the Harris criterion is able to explain why quenched disorder is relevant for continuous absorbing phase transitions.

Conversely, the Imry-Ma [15] and Aizenman-Wehl [16] criteria establish that quenched disorder suppresses the phase coexistence in equilibrium systems for $d \leq 2$. In the last decades, it was shown [18–20] that the discontin-

uous transition in the Ziff-Gulari-Barshad (ZGB) model becomes continuous when the disorder strength is large enough. Afterwards, recent results have extended the above conjectures for (discontinuous) absorbing phase transitions, suggesting that they also become rounded in the presence of quenched disorder for $d \leq 2$, irrespectively the disorder strength [9].

Although less studied than the spatial disorder, the influence the temporal disorder has also been considered in some cases [17, 21, 22]. Unlike the quenched case, the control parameter becomes time-dependent, resulting in a temporarily active (ordered) as well as absorbing (disordered) phases, whose effect of variability becomes pronounced at the emergence of the phase transition. In particular, the (few) available results have shown that temporal disorder is highly relevant perturbation [23], suppressing the DP phase transitions in all dimensions. For systems with up-down symmetry they are relevant only for $d \geq 3$. *Temporal* Griffiths phases (TGPs), a region in the active phase characterized by power-law spatial scaling and generic divergences of the susceptibility have also been reported for some systems [21, 23], but not found in low dimensional systems with up-down symmetry [22]. On the other hand, the effect of temporal disorder for discontinuous absorbing phase transitions is still unknown.

In order to shed some light in this direction, here we tackle the effect of temporal disorder in low dimensional discontinuous absorbing transition models. Our study aims to answer three fundamental questions: (i) is the occurrence of phase coexistence forbidden under the presence of (temporal) disorder? (ii) if no, which changes does it provoke with respect to the pure (without disorder) version? (iii) Does the temporal disorder induces temporal Griffiths phases around these phase transitions? These ideas will be tested in three models yielding un-

doubtedly discontinuous absorbing phase transitions in bidimensional and infinite-dimensional systems, namely the ZGB model for CO oxidation [24] and two lattice versions of the second Schlögl model (SSM) [12, 25]. As shall be shown further, in all models the phase transition are signed by a behavior similar to their pure (without disorder) counterparts, including bistability around the coexistence point and common finite size scaling behavior with the inverse of the system volume, as recently proposed in [28].

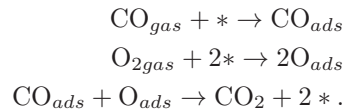
This paper is organized as follows: In Sec. II we present the studied models and all described methods. Results are shown in Sec. III and conclusions are drawn in Sec. IV.

II. MODELS AND METHODS

The SSM is sketched by the reactions $2A \rightarrow 3A$ and $A \rightarrow 0$ occurring with transition rates λ and μ , respectively. The origin of a discontinuous transition, by means of above rules, can be heuristically understood under a mean-field treatment. The former reaction predicts a particle growth following a quadratic dependence on the density, which makes low-density (active) state becoming unstable and thus, a jump to a nonzero (large) density arises as the creation probability $\lambda/(\lambda + \mu)$ increases to a threshold value $\lambda = 4\mu$ [1]. On the other hand, by taking above rules in a regular lattice, the system dimensionality and a minimal neighborhood of two adjacent particles to an empty site (in order to fill the reaction $2A \rightarrow 3A$) are essential ingredients for the emergence of a phase coexistence [26]. In other words, an empty site has to be a minimal number of two adjacent particles to be occupied by a new species. Here, we consider two lattice versions of the SSM. The former, proposed by Jensen et al. [27] and afterwards reconsidered in Ref. [9] is defined as follows: For fixed $\mu = \alpha$ and $\lambda = 1$ a given particle is randomly selected and with probability $p_a^0 = \alpha/(\alpha + 1)$ it is annihilated. With the complementary probability $1 - p_a^0$, a nearest neighbor site is chosen. If this latter is empty, the selected particle diffuses to it, and otherwise an offspring particle is created at a randomly chosen neighboring site with probability p_b provided it was empty; otherwise nothing happens. The value $p_b = 0.5$ has been considered in similarity with the previous studies [9, 27, 28]. The latter SSM version is similar to the previous one, but unlike it, the particle diffusion is forbidden. In particular, the annihilation particle (performed with probability p_a^0) and the choice of nearest neighbor site (with complementary probability) are identical to the first SSM. However, whenever the latter subprocess is chosen and the adjacent site is empty, its number of nearest occupied sites nn will be evaluated. A new offspring will be created with rate $nn/4$ if $nn \geq 2$. No particle creation occurs if $nn \leq 1$. In both SSMs, the system density ρ is the order parameter and an active-absorbing (discontinuous) transitions occur at

$\alpha_0 = 0.0824(1)$ [28, 29] and $\alpha_0 = 0.2007(6)$ [30], for the former and latter versions respectively.

The third investigated system is the ZGB model [24], which qualitatively reproduces some features of the oxidation of carbon monoxide on a catalytic surface. The surface is modelled as a square lattice, in which each site can be empty (*), or occupied by an oxygen (O_{ads}) or a carbon monoxide (CO_{ads}). It is summarized by the following reactions:



In practice, molecules of CO_{gas} and O_{2gas} hit the surface with complementary probabilities Y and $(1 - Y)$, respectively whenever the chosen site is empty. At the surface, O_2 molecule dissociates in two independent O atoms, each one occupying two adjacent empty sites. At any time, if a $CO_{ads}O_{ads}$ pair is placed at neighbouring sites on the surface, a CO_2 molecule is formed and desorbs (instantaneously), leaving both sites empty.

By changing the parameter Y , the model exhibits two phase transitions between an active steady state and absorbing (“poisoned”), in which the surface is saturated either by O or by CO. The O-poisoned transition is found to be continuous. On the other hand, since O_2 can adsorb only at rare vacant pairs on a lattice with high-CO coverage, such configurations are unstable to complete CO saturation. Therefore the CO-poisoned transition is strongly discontinuous. Here we focus on such latter phase transition.

Except in one case (to be explained further), the temporal disorder is implemented as follows: As the computational time changes by $\Delta t = t^*$, a new value for the control parameter is extracted from a uniform distribution with mean p_0 and width σ . More specifically, $p(t)$ is given by $p(t) = p_0 + (2\xi - 1)\sigma$, being ξ a random number drawn from a uniform distribution with $\xi \in [0, 1]$. For the SSM the complementary annihilation probability reads $p_0 = 1 - p_a^0 = \frac{1}{1+\alpha}$, whereas p_0 corresponds to the reaction rate Y for the ZGB.

For locating the transition point and the classification of phase transition, we consider three alternative procedures. In the first, the time behavior of the order parameter, starting from a fully active initial configuration, is considered. In the case of discontinuous absorbing phase transitions, the transition point can be estimated through a threshold value $\tilde{\alpha}$ that separates endless activity from an exponential convergence to the absorbing phase [26, 31, 32]. In this case, the absence of a power law behavior separating the activity from the extinction can be used as a rough indicator of a discontinuous phase transition. Alternatively, a more reliable analysis is achieved by performing a finite-size treatment, as that proposed recently in Ref. [28]. According to it, the difference between the pseudo-transition point α_L and the transition point α_0 scales with L^{-2} , where L^2 denotes

the system volume (in the bidimensional case). The estimation of α_L can be done under different ways, such as the peak of system variance $\chi = L^2(\langle \rho^2 \rangle - \langle \rho \rangle^2)$ or even through the value in which the bimodal order parameter distribution presents two equal areas [28]. However, such scaling behavior is verified only by considering some kind of quasi-stationary (QS) ensemble, i.e. an ensemble of states accessed by the original dynamics at long times *conditioned on survival* (restricted to those are not trapped into an absorbing state). Here we employ an efficient numerical scheme given in Ref. [33], in which configurations are stored and gradually updated during the evolution of the stochastic process. Whenever a transition to the absorbing state is imminent, the system is “relocated” to one of the saved configurations. This accurately reproduces the results from the much longer procedure of performing averages only on samples that have not been trapped in the absorbing at the end of their respective runs. The intensive quantities in a QS ensemble must converge to the stationary ones when the system size $L \rightarrow \infty$. In the third analysis, the mean survival time τ is considered for different system sizes. According to Refs. [9, 34], the coexistence point is the separatrix of an exponential growth of τ and an exponential increase until $L < L_c$ followed by a decreasing behavior for $L > L_c$. Since the behavior of τ has not been established yet, we shall also quantify it, in order to compare with the pure (not disordered) cases.

III. RESULTS AND DISCUSSION

A. Models in a square lattice

The first analysis over the influence of temporal disorder is achieved by inspecting the time decay of system density $\rho(t)$ starting from a fully active initial configuration. For the first SSM Figs. 1 and 2 (panels (a)) show $\rho(t)$ for $\rho_0 \equiv \rho(0) = 1$ for the pure versions, $\sigma = 0.05$ (not shown) and $\sigma = 0.15$ with $\Delta t = 1$ respectively.

As mentioned previously, in all cases there is a threshold value $\tilde{\alpha}$ separating indefinite activity and exponential decay toward the particle extinction. In addition, the $\tilde{\alpha}$'s are strongly dependent on σ and occur at $\tilde{\alpha} = 0.0812, 0.076$ (not shown) and 0.035 for the pure, $\sigma = 0.05$ and 0.15 , respectively. By repeating above analysis for distinct initial configurations (panels (b)) with distinct densities ρ ($10^{-2} \leq \rho_0 \leq 1$), the curves converge to two well defined stationary states, with $\rho \ll 1$ and $\rho \sim \rho^*$, signalling the bistability of active and absorbing phases, reinforcing in all cases a first-order phase transition. For the pure, $\sigma = 0.05$ and 0.15 , ρ^* read $0.637(2)$, $0.63(2)$ and $0.77(2)$ respectively.

Inspection of quasi-steady properties for distinct L 's reveal that the α_L 's (panels (c) and (d)), in which the order parameter variance χ is maximum, scales with $1/L^2$ and gives $\alpha_0 = 0.0824(2)$, $0.0823(2)$ (not shown) and $0.0680(2)$ for the pure, for $\sigma = 0.05$ (not shown) and 0.15 ,

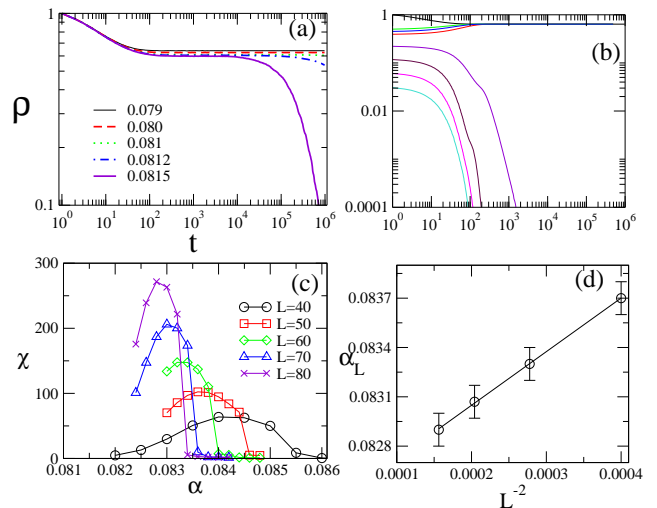


FIG. 1: (**Color online**): Results for the pure first SSM. Panel (a) shows the time decay of ρ for a uniform initial condition and distinct values of α . Panel (b) shows the bistable behavior of ρ close to the separatrix point $\tilde{\alpha} \sim 0.0815$ for distinct initial densities ρ_0 ranging from 10^{-2} to 1. Panel (c) and (d) shows the order parameters variance χ versus α and the α_L , in which χ is maximum, vs $1/L^2$.

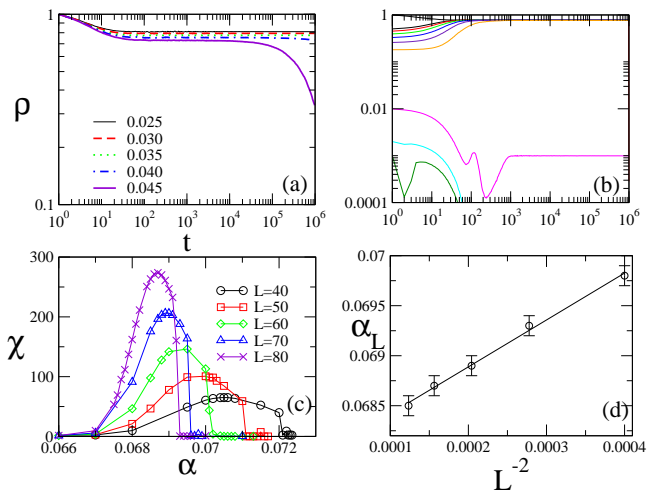


FIG. 2: (**Color online**): Results for $\sigma = 0.15$. Panel (a) shows the time decay of ρ for a uniform initial condition $\rho(0) = 1$ and distinct values of α . Panel (b) shows the bistable behavior of ρ at $\tilde{\alpha} \sim 0.035$ for distinct initial densities ranging from 10^{-2} to 1. Panel (c) and (d) shows the order parameters variance χ versus α and the α_L , in which χ is maximum, vs $1/L^2$.

respectively. In particular for $L = 100$, the peak in χ yields at $0.0827(1)$, $0.0826(1)$ and $0.0684(1)$, respectively. Therefore, both previous analyses suggest that temporal disorder does not forbid a discontinuous phase transition. However, it induces the increase the metastable region at the emergence of the phase coexistence, i.e. $\alpha_L - \tilde{\alpha}$ increases with σ . This feature shares similarities with some procedures studied for characterizing the first-order tran-

sition in the ZGB and allied models close to the coexistence by taking different initial configurations [35].

An important point concerns that above transition points decrease substantially by increasing σ , revealing the suppression (absence) of phase transition for $\sigma > 0.22$, which is a rather small disorder strength. In order to strengthen (e. g. to increase) the influence of disorder in the first SSM, first we increase the Δt , in which the occurrence of rare effects induced by the disorder are expected to be increased [36]. Since no larger values of σ is possible for the SSM, only in such case we take a bimodal disorder distribution, in which the annihilation rate is chosen from two values, α and 20α , with rates \bar{p} and $1 - \bar{p}$, respectively. Results are shown in Fig. 3 (a) – (b) for $\bar{p} = 0.2$ and $L = 200$. Second, the analysis of second SSM for $\sigma = 0.4$ (with $\Delta t = 1$) is considered. Since its pure version yields a larger transition point, it is possible to increase substantially the σ (in contrast to the first SSM). Results are shown in Fig. 3 (panels (c) and (d)).

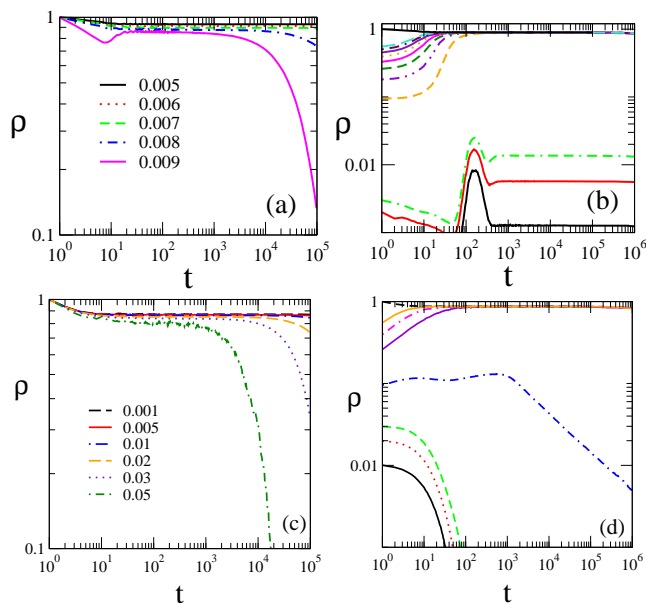


FIG. 3: (**Color online**): For the first SSM with bimodal temporal disorder distribution, panel (a) shows log-log temporal decay of ρ for distinct α 's for $\Delta t = 6$. Panel (b) shows the bistable behavior of ρ at $\alpha = 0.007$ (very close to separatrix point $\tilde{\alpha} \sim 0.008$) for distinct initial densities ρ_0 ranging from 10^{-3} to 1. Panel (c) shows the same analysis in (a), but for the second SSM with uniform distribution for $\sigma = 0.4$ and $\Delta t = 1$. In (d), the bistable behavior of ρ at $\alpha = 0.001$, close to the transition point $\tilde{\alpha} \sim 0.005$, for distinct initial densities ranging from $\rho_0 = 10^{-3}$ to 1.

In both systems, the phase transitions obey the same pattern than previous cases: Separatrix points $\tilde{\alpha} \sim 0.008$ ($\tilde{\alpha} \sim 0.005$) and bistable behaviors of $\rho(t)$ at the vicinity of transition points [exemplified here for $\alpha = 0.007$ (and $\alpha = 0.001$)]. In both cases, the fact of separatrix points occurring for very small α 's evidences the relevance of disorder. As for the first SSM, the phase transition is

suppressed for sufficient large σ 's, whose results reveal the absence of phase transition for $\sigma > 0.4$.

Now, we turn our attention to the ZGB model. In Fig. 4 and Fig. 5 we show the results for disorder strengths $\sigma = 0.05$ and $\sigma = 0.10$, respectively. In particular, we have considered rather small disorder strengths, in order not to "mix" both phase transitions. In both cases, similar results to the SSM have been obtained. Panels (a) show once again the onset point \tilde{Y} separating activity from a exponential growth toward a full carbon monoxide poisoning. The \tilde{Y} 's decreases by raising the disorder parameter σ , reading $\tilde{Y} = 0.527(1)$, $0.523(1)$, $0.516(1)$ and $0.500(2)$ for the pure, $\sigma = 0.05$, 0.1 and 0.2 (not shown), respectively. In addition, Y_L 's, obtained from the maximum of order parameter variance χ scales with $1/L^2$ as seen in the pure version [28]. For the pure, $\sigma = 0.05$, 0.1 and 0.2 (not shown) we obtain $Y_0 = 0.5253(3)$, $0.524(1)$, $0.520(1)$ and $0.509(2)$, respectively. Although less pronounced than for the previous example, note that the difference $Y_0 - \tilde{Y}$ increases with σ , reinforcing that disorder increases the spinodal region around the phase coexistence.

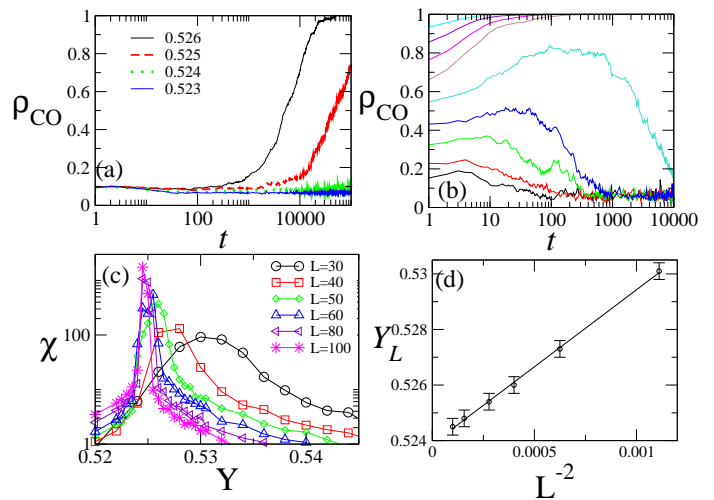


FIG. 4: (**Color online**): Results for the ZGB model for $\sigma = 0.05$. Panel (a) shows the time decay of ρ_{CO} for a uniform initial condition ($\rho_{CO}(0) = 0$) and distinct values of Y . Panel (b) shows the bistable behavior of ρ_{CO} for $Y = 0.522$ for distinct initial densities $0.1, 0.2, \dots, 0.9$ (Linear system size: $L = 800$). Panel (c) and (d) shows the order parameters variance χ versus Y and the Y_L , in which χ is maximum, vs $1/L^2$.

Fig. 6 shows the mean lifetime of the QS state (defined as the time between two absorbing attempts during the QS regime), for the pure and disordered systems. We observe in all cases the same behavior (in similarity with Ref. [9]): a threshold value separating exponential growth of τ from a increasing until a maximum system size L_c followed by a decrease of τ for $L > L_c$. For the pure cases, from such analysis the coexistence point is located within the interval $0.0805 < \alpha < 0.081$ (SSM) and $0.5256 < Y < 0.5258$ (ZGB). In the presence of tempo-

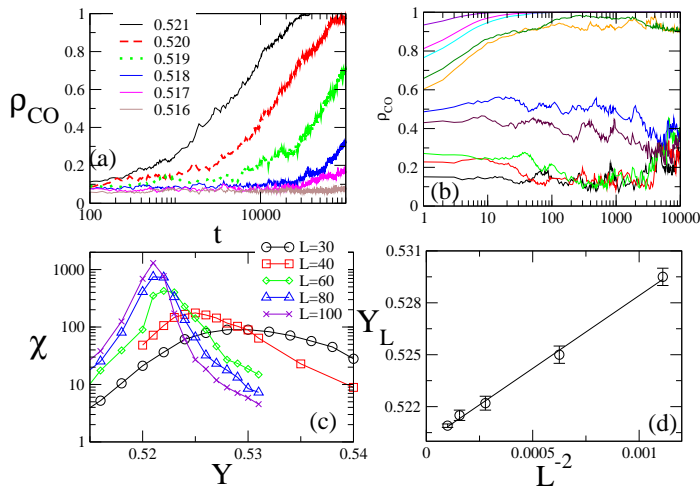


FIG. 5: (**Color online**): Results for the ZGB model for $\sigma = 0.10$. Panel (a) shows the time decay of ρ_{CO} for a uniform initial condition ($\rho_{CO}(0) = 0$) and distinct values of Y . Panel (b) shows the bistable behavior of ρ_{CO} for $Y = 0.520$ for distinct initial densities 0.1, 0.2, ..., 0.9 (Linear system size: $L = 800$). Panel (c) and (d) shows the order parameters variance χ versus Y and the Y_L , in which χ is maximum, vs $1/L^2$.

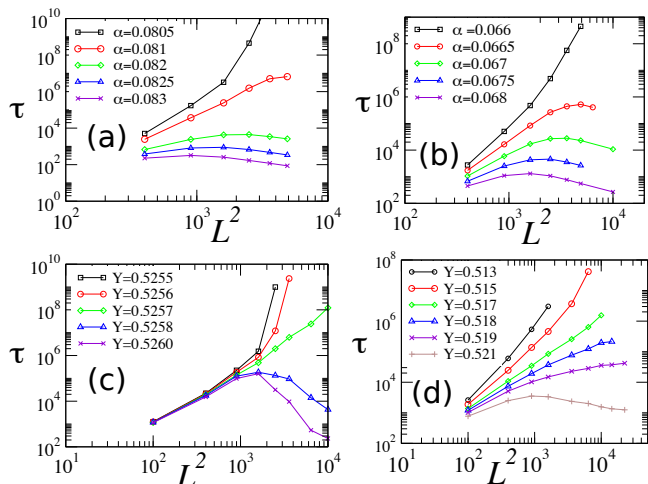


FIG. 6: (**Color online**): For the SSM (ZGB) model, panels (a)[(c)] and (b)[(d)] show the QS lifetime for the pure and disordered versions, respectively. In the latter case, we take $\sigma = 0.15$ and 0.1 for the SSM and ZGB models, respectively.

ral disorder, the crossover of regimes are in the interval $0.066 < \alpha < 0.067$ ($\sigma = 0.15$) and $0.515 < Y < 0.518$ ($\sigma = 0.1$), respectively, which agrees with previous estimates obtained from the maxima of χ . Thus all above findings suggest that in contrast with systems exhibiting temporal Griffiths phases (TGP), τ does not grow algebraically within a region the active phase. These results are similar to those obtained for the generalized voter model [22], suggesting that in analogy with the discontinuous transition, the absence of TGPs could be related

to the (low) dimensionality. Thus, the present results for discontinuous absorbing transitions reinforce a general property of TGPs not appearing in low-dimensional systems, where standard fluctuations dominate over temporal disorder.

We close this section by remarking that in contrast to the SSM (at least until for $\sigma = 0.4$), the discontinuous active-CO poisoned transition exhibits a behavior consistent to a continuous transition for $\sigma > 0.3$ (not shown). Thus, in contrast to the SSM (at least until $\sigma \leq 0.4$) numerical results indicate that the increase of σ suppress the phase coexistence.

B. Models in a complete graph

Aimed at investigating the effects of temporal disorder infinite-dimensional structures, in the last analysis we consider a mean-field like description of both above models, through their analysis in a complete graph (CG). In this treatment, each site interacts with all others, so that an exact analysis is allowed. For the SSM, besides the reactions $A \rightarrow 0$ and $2A \rightarrow 3A$, one takes the coagulation process $2A \rightarrow A$ occurring with rate ν [9, 38]. The discontinuous transitions yield at the exact points $\alpha = 1/(2\sqrt{\nu})$ and $Y = 2/3$ [37, 38], for the SSM and ZGB, respectively. In particular for latter case, due to the prohibition against C-CO occupying nearest-neighbor pairs, only one species (CO or O) may be present at any moment. Let $\rho = \rho_{CO} - \rho_O$ with ρ_{CO} and ρ_O the fraction of sites bearing a CO and O, respectively. Therefore we can describe a system of N sites completely by a single variable, with $\rho = -1$ representing the O-poisoned state and $\rho = 1$ the CO-poisoned state (see more details in [37]). In particular, we take $\nu = 1$ for the SSM and in all cases the temporal disorder was introduced in a similar way to that considered in Sec. II.

Results for ρ for the SSM and ZGB models are shown in panels (a) of Figs. 7 and 8, respectively. In both cases, analysis in the complete graph predicts similar behavior to that observed on square lattices: the reduction of the active region, when compared to their pure counterparts and occurrence of bimodal probability distributions [see e.g panels (c)-(d) in Figs. 7 and 8]. In particular, for disorder strenght $\sigma = 0.1$, the transition points are shifted from $\alpha = 0.5$ to $\alpha = 0.475$ (SSM), and from $Y = 2/3$ to $Y = 0.635$ (ZGB). Thus, for lower σ 's, the inclusion of (low) disorder maintain the phase coexistence. However, by increasing σ the active phase peaks become broader, suggesting the appearance to a continuous transition as shown in Fig. 9 (a) and (b). Despite this, there are some differences when compared to their low dimensional counterparts. In particular, there is a region in the active phase (see e.g Fig. 9 (c) and (d)), with the control parameter X in the range $X_c < X < X_c + \sigma$, in which τ grows slower than exponential, and then it saturates at a finite value. Such behavior is related to the abrupt transition that occurs when the noise takes the control param-

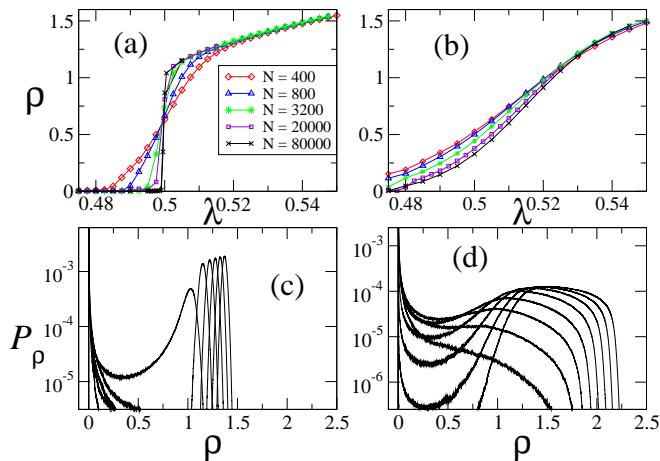


FIG. 7: (**Color online**): For the SSM on a complete graph, the QS density ρ for the pure model (a) and with temporal disorder strength $\sigma = 0.1$ (b). In (c), the QS probability distributions for the pure model, with α ranging from 0.475 to 0.525. In (d), the QS probability distributions for $\sigma = 0.1$, and α ranging from 0.4750 to 0.5625 (System size: $N = 10000$ in (c) and (d)).

eter to a value that drives the system to the absorbing state. Since configurations with intermediary densities are unstable in these systems, one observes a bimodal QS probability distribution in this region. It is important to highlight that this behavior is remarkably distinct from a temporal Griffiths phase, which is characterized by an algebraic growth of τ and until now has been observed only in systems exhibiting continuous phase transitions into absorbing states subject to temporal disorder.

IV. CONCLUSIONS

The influence of temporal disorder has been investigated in the context of discontinuous absorbing phase transitions. Three models have been extensively studied under three distinct numerical procedures. Our results strongly suggest that in contrast to the spatial disorder, discontinuous absorbing transitions are not forbidden by the presence of temporal disorder in low dimensional systems. In particular, the behavior of quantities in low-dimensional systems are similar to their pure counterparts. However, the temporal disorder induces an increasing of metastable region close to phase coexistence. Results suggest that the existence of so called temporal Griffiths phases (TGP) is not presented in bidimensional systems. Some remarks over the existence of TGPs are in order: Earlier results for different systems have shown that the inclusion of temporal disorder does not necessarily lead to the presence of TGPs [21, 22]. Although

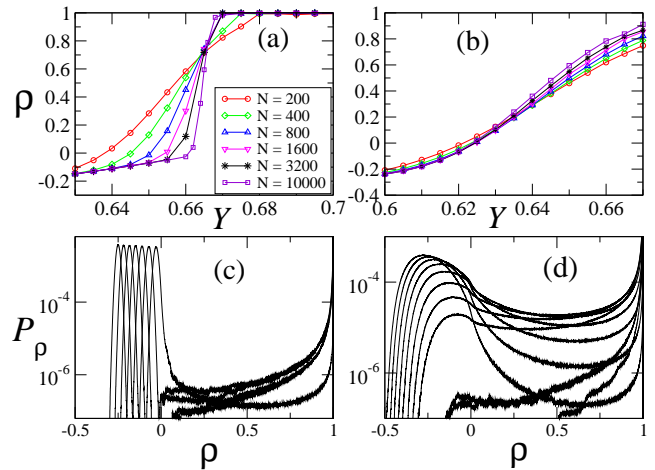


FIG. 8: (**Color online**): For the ZGB model on a complete graph with Y ranging from 0.60 to 0.70 and $N = 10000$, the QS ρ_{CO} for the pure model (a) and with temporal disorder strength $\sigma = 0.1$ (b). In (c) and (d), the QS probability distributions for the pure model and for $\sigma = 0.1$, respectively.

it suppresses the DP universality class in all dimensions, TGPs can not be presented in $d = 1$, depending the way the disorder is introduced. Similar conclusions are also verified in distinct up-down systems, in which only for $d \geq 3$ they are presented. Thus all these cases claim that the dimensionality plays an important role for the manifestation of TGPs, in which standard fluctuations (induced by the dimensionality) are not expected to dominate over temporal disorder.

On the other hand, we observed that in the infinite-dimensional models the discontinuous transitions are also manifested but they become more rounded by increasing the disorder and there is an a region in the active phase in which the lifetime of the QS state grows slower than exponential, and then it saturates at a finite value.

A very important point concerns that our results does not exclude a discontinuous transition becoming continuous above a disorder threshold σ_c in the bidimensional case. Since for the SSMs the transition points decreases substantially as σ increases, we have not verified the crossover to a continuous transition at least until $\sigma = 0.4$, despite results for $d \rightarrow \infty$ point out in this direction. On the other hand, for the ZGB model, a behavior indicating a continuous transition has been obtained for $\sigma > 0.3$, suggesting that the temporal disorder suppresses the original discontinuous transition. Also, results for an one-dimensional (absorbing) discontinuous transition example reveals clearly the suppression the phase coexistence for larger temporal disorder strengths [39].

Possible extension of this work include studies of the effect of temporal correlated disorder and the more general case of spatio-temporal disorder, i.e. how the discontin-

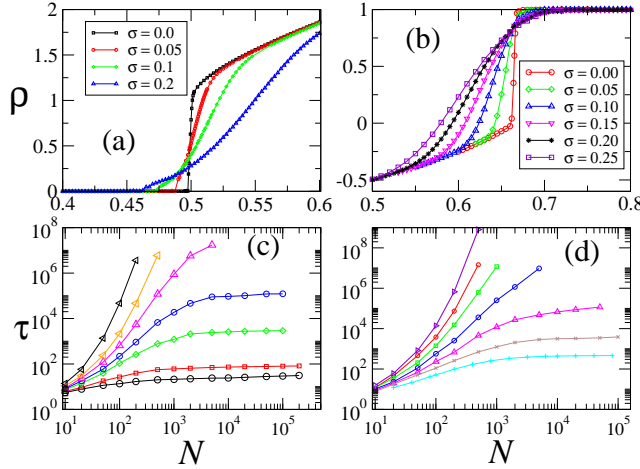


FIG. 9: (**Color online**): QS density ρ for (a) the SSM model on a complete graph and (b) for the ZGB model with distinct σ and $N = 10000$. (c) Lifetime of the QS state for the SSM model on a complete graph for $\sigma = 0.1$, and $\alpha = 0.500, 0.510, 0.520, 0.525, 0.530, 0.535$, and 0.545 from bottom to top. (d) Lifetime of the QS state for the ZGB model for $\sigma = 0.1$ and $Y = 0.55, 0.56, 0.57, 0.58, 0.59, 0.60$ and 0.61 , from top to bottom.

uous phase transition is affected by an external perturbation that fluctuates in both space and time [40]. Both cases appear to be of particular interest in the context of ecosystems, where the effects of noise on the extinction of a population due to environmental changes have been attracting considerable attention recently [41]. Also, extension of both models for larger dimensions are intended to be investigated, in order to confirm above hypothesis.

-
- [1] J. Marro and R. Dickman, *Nonequilibrium Phase Transitions in Lattice Models* (Cambridge University Press, Cambridge, 1999).
- [2] H. Hinrichsen, *Adv. Phys.* **49**, 815 (2000).
- [3] G. Ódor, *Rev. Mod. Phys.* **76**, 663 (2004).
- [4] M. Henkel, H. Hinrichsen and S. Lubeck, *Non-Equilibrium Phase Transitions Volume I: Absorbing Phase Transitions* (Springer-Verlag, The Netherlands, 2008).
- [5] G. M. Buendia and P. A. Rikvold, *Phys. Rev. E* **88**, 012132 (2013).
- [6] V. Bustos, R. O. U nac, and G. Zgrablich, *Phys. Rev. E* **62**, 8768 (2000).
- [7] D.-J. Liu, X. Guo, and J. W. Evans, *Phys. Rev. Lett.* **98**, 050601 (2007).
- [8] C. Buono, F. Vazquez, P. A. Macri, and L. A. Braunstein *Phys. Rev. E* **88**, 022813 (2013).
- [9] P. Villa Martín, J. A. Bonachela and M. A. Muñoz, *Phys. Rev. E* **89**, 012145 (2014).
- [10] M. M. de Oliveira, S. G. Alves and S. C. Ferreira, *Phys. Rev. E* **93**, 012110 (2016).
- [11] J. Hooyberghs, F. Igloi, and C. Vanderzande, *Phys. Rev. Lett.* **90**, 100601 (2003).
- [12] M. M. de Oliveira and S. C. Ferreira, *J. Stat. Mech.* **2008**, P11001 (2008).
- [13] See for example, T. Vojta and M. Dickison, *Phys. Rev. E* **72**, 036126 (2005); H. Barghathi and T. Vojta, *Phys. Rev. Lett* **109**, 170603 (2012).
- [14] A. B. Harris, *J. Phys. C* **7**, 1671 (1974).
- [15] Y. Imry and S.-k. Ma, *Phys. Rev. Lett.* **35**, 1399 (1975).
- [16] M. Aizenman and J. Wehr, *Phys. Rev. Lett.* **62**, 2503 (1989).
- [17] I. Jensen, *Phys. Rev. Lett.* **77**, 4988 (1996).
- [18] J.-P. Hovi, J. Vaari, H.-P. Kaukonen, and R.M. Nieminen, *Comput. Mater. Sci.* **1**, 33 (1992).
- [19] J. Cortés and E. Valencia, *Surf. Sci.* **425**, L357 (1999).
- [20] G. L. Hoenicke and W. Figueiredo, *Phys. Rev. E* **62**, 6216 (2000).
- [21] F. Vazquez, J. A. Bonachela, C. López and M. A. Muñoz, *Phys. Rev. Lett.* **106**, 235702 (2011).
- [22] R. Martínez-García, F. Vazquez, C. López, and M. A. Muñoz, *Phys. Rev. E* **85**, 051125 (2012).
- [23] J. A. Hoyos and T. Vojta, *Europhysics Lett.* **112**, 30002 (2015).
- [24] R. M. Ziff, E. Gulari, and Y. Barshad, *Phys. Rev. Lett.* **56**, 2553 (1986).
- [25] F. Schlögl, *Z. Phys.* **253**, 147 (1972).
- [26] C. E. Fiore, *Phys. Rev. E* **89**, 022104 (2014).
- [27] A. Windus and H. J. Jensen, *J. Phys. A* **40**, 2287 (2007).
- [28] M. M. de Oliveira, C. E. Fiore and M. G. E. da Luz *Phys. Rev. E* **92**, 062126 (2015).
- [29] In fact, our estimate is different to the estimate $\alpha_c = 0.0742(1)$ [28], as a result of a slightly different dynamics implementation.
- [30] E. F. da Silva and M. J. de Oliveira, *Comp. Phys. Comm.* **183**, 2001 (2012).
- [31] S. Pianegonda and C. E. Fiore, *J. Stat. Mech.* 2015, P08018 (2015).
- [32] S. Pianegonda and C. E. Fiore, *Physica A* **451**, 349

- (2016).
- [33] M. M. de Oliveira and R. Dickman, Phys. Rev. E **71**, 016129 (2005); Braz. J. Phys. **36**, 685 (2006).
- [34] S. Tanase-Nicola and D. K. Lubensky, Phys. Rev. E. **86**, 040103 (2012).
- [35] J. W. Evans and M. S. Miesch, Surf. Sci. **245**, 401 (1991).
- [36] H. Barghathi, T. Vojta and J. A. Hoyos, arXiv:1603.08075.
- [37] M. M. de Oliveira and R. Dickman, Physica A **343**, 525 (2004).
- [38] R. Dickman and R. Vidigal, J. Phys. A **35**, 1147 (2002).
- [39] C. E. Fiore and M. M. de Oliveira (in progress).
- [40] T. Vojta and R. Dickman, arXiv:1601.03282v1 (2016).
- [41] O. Ovaskainen and B. Meerson, Trends in Ecology & Evolution **25**, 643 (2010).